Excellent Compatibility of Solvate Ionic Liquids with Sulfide Solid Electrolytes: Toward Favorable Ionic Contacts in Bulk-Type All-Solid-State Lithium-Ion Batteries

*Dae Yang Oh, Young Jin Nam, Kern Ho Park, Sung Hoo Jung, Sung-Ju Cho, Yun Kyeong Kim, Young-Gi Lee, Sang-Young Lee, and Yoon Seok Jung**

Rechargeable lithium batteries can achieve the high energy densities required for high-performance energy storage.[1,2] Inorganic solid electrolytes (SEs) are key components in the development of alternative types of rechargeable lithium batteries such as all-solid-state Li batteries (ASLBs)[3–5] and aqueous Li batteries[6–8] (e.g., aqueous Li–O_2 batteries[7] and Li–iodine batteries.[8]) The "hybrid" configuration of aqueous Li batteries, which have high energies and power densities, is possible because of the use of inorganic SE films such as the Na superionic conductor (NASICON)-type $Li_{1+x+y}Al_x(Ti,Ge)_{2-x}Si_yP_{3-y}O_{12}$ (Ohara Inc.)[9] and the garnet-type $Li_7La_3Zr_2O_{12}$ (LLZO).[10] However, it is challenging to maintain stability at the interface of the SE and aqueous phase during long-term operation.[11]

More importantly, the use of inorganic SEs can lead to ultimate safety by developing ASLBs.[3–5] This is of prime importance if the application of lithium batteries is to expand to large-scale energy storage such as electric vehicles (EVs) and energy storage systems.[1,5] ASLBs also offer promise in achieving superior energy densities to that of the conventional lithium-ion batteries (LIBs). This is possible because the voltage of an ASLB can be increased by simply stacking the monocells together (in contrast to conventional LIBs, which need serial connections between fully packaged monocells),[12] by adopting advanced electrode chemistries (e.g., sulfur), using nanostructures,[5,13–15] or by engineering the electrolyte into architectures.[12] ASLBs can be classified into two types: thin-film[16] and bulk-type.[3,5,13–15] However, large-scale application of the thin-film-type ASLBs involves a prohibitively expensive manufacturing process that uses a vacuum deposition process, reducing its practicability.[16] In contrast, as the building units, the active materials, the SE, and the conductive additives, are all powders, the bulk-type ASLBs are considered highly competitive in terms of scalable production and high energy density.[5]

A prerequisite for the realization of bulk-type ASLBs is that the SE has a high ionic conductivity. The oxide SEs such as LLZO,[10] LATP,[9] $Li_{3x}La_{2/3-2x}\square_{1/3-2x}TiO_3$ (LLTO)[17] have sufficiently high ionic conductivities at room temperature (>10^{-4} S cm^{-1}), and have excellent stability in air.[9,10,17] However, the most challenging barrier to using these oxide SEs for bulk-type ASLBs is a difficulty in making favorable contacts between SE and active materials.[4] Sintering at elevated temperatures of at least 800 °C is inevitable,[18] which disrupts the interfaces and results in extremely poor performances.[19,20] In sharp contrast, using sulfide materials as the SE offers a critically important property: ductility (the Young's modulus of the sulfide SE lies in the range between organic polymers and oxide ceramics), which enables 2D contacts with active materials by simple cold-pressing.[21] Furthermore, extremely high ionic conductivities (approaching that of organic LEs (≈10^{-2} S cm^{-1})) have been achieved by using several state-of-the-art sulfide materials such as $Li_{10}GeP_2S_{12}$ (LGPS, 12 mS cm^{-1}),[3] $Li_{10}SnP_2S_{12}$ (4 mS cm^{-1}),[22] and Li_2S–P_2S_5 (e.g., $Li_7P_3S_{11}$ or $70Li_2S$–$30P_2S_5$: 17 mS cm^{-1} at maximum).[23,24] Despite the evolution of harmful H_2S gas when sulfide SEs are in contact with the moisture in air,[25,26] and their relatively poor oxidation stability,[5,27] the fascinating properties of sulfide SEs (ductility and high ionic conductivities) have led to explosive interest in the development of bulk-type ALSBs.[5]

For ASLBs and aqueous Li batteries, the interface at which heterogeneous species are in contact is critical and governs battery performance. Cold-pressing can deform the sulfide SE easily, allowing the formation of 2D contacts with the active materials. But, the fabrication of a completely poreless monolith in which completely intimate contacts are formed is difficult,[12] and there is clearly room for improvement. In the literature, the specific capacities of ASLBs appear to be much lower than those obtained by the LE cells.[5,28,29] For example, $Li_4Ti_5O_{12}$ (LTO) exhibits a reversible capacity of ≈80 mA h g^{-1} in ASLBs (theoretical capacity: 175 mA h g^{-1}).[29] Even worse is the commercially available $LiFePO_4$ (LFP) with sulfide SEs, and which showed a capacity of only ≈40 mA h g^{-1} between 2.0 and 4.7 V (vs Li/Li^+) at 6.4 μA cm^{-2} (=1.3 mA g_{LFP}^{-1}) at 50 °C.[28] In this regard, a reasonable approach to increase performance of ASLBs would be the inclusion of a small amount of a soft or liquid-state Li-ion conductive organic components,

D. Y. Oh, Y. J. Nam, S. H. Jung, S.-J. Cho, Y. K. Kim, Prof. S.-Y. Lee, Prof. Y. S. Jung
School of Energy and Chemical Engineering
Department of Energy Engineering
Ulsan National Institute of Science and Technology (UNIST)
Ulsan 689-798, South Korea
E-mail: ysjung@unist.ac.kr
K. H. Park
School of Chemical and Biological Engineering
Seoul National University
599 Gwanangno, Gwanak-gu, Seoul 151-742, South Korea
Dr. Y.-G. Lee
Power Control Device Research Team
Electronics and Telecommunications Research Institute (ETRI)
218, Gajeongno, Yuseong-gu, Daejeon 305-700, South Korea

DOI: 10.1002/aenm.201500865

in the composite electrode of ASLBs to assist in the formation of ionic contacts. However, there are no reports on the operation of sulfide-based ASLBs using organic LEs. This may be because of the highly reactive nature of the lithium-containing sulfide materials toward the organic solvents used in conventional LEs, for example, in the cases of $LiTi_2(PS_4)_3$[30] and the Li polysulfides.[7]

In the development of "hybrid" ASLBs, a question arises: are there any solvents that show no reactivity with the sulfide SE and are safe? Also, these solvents must also being able to dissolve Li salts well enough to give sufficiently high ionic conductivity. At first glance these requirements appear contradictory. The question led us to recent research addressing polysulfide dissolution in Li–S batteries by using alternative LEs.[31–33] The nonsolvent behavior of several high-concentration LEs toward lithium polysulfides is reported.[31–33] For example, glyme-based LEs. As the ratio of salt to solvent increases, a threshold is reached where a solvent–salt complex (also named as solvate ionic liquids (SIL)) is formed. At this composition, unique room temperature ionic liquid (RTIL)-like behaviors were observed.[34–36] The SILs such as $Li(glyme)_yX$ (X: polyanion)[33] and Li(acetonitrile (AN))$_2$[bis(trifluoromethanesulfonyl)imide (TFSI)][31] have been shown to suppress the dissolution of lithium polysulfides, resulting in excellent performance in Li–S batteries. In addition, the superior safety properties (nonflammability, low volatility, and excellent thermal stability) of ionic liquids compared to the conventional LEs should be noted.[31–36]

In this report, which is based on the previously discussed research and motivation, we report, for the first time, the excellent stability of sulfide SEs toward solvate ionic liquids and demonstrate their application in high-performance ASLBs.

For a systematic assessment of the reactivity of glyme-based liquids toward sulfide SEs, three liquid samples of pure triglyme (triethylene glycol dimethyl ether, G3), $Li(G3)_4TFSI$ (hereafter referred to as "$Li(G3)_4$"), and Li(G3)TFSI (hereafter referred to as "LiG3") were prepared. For the sulfide SEs, Li_3PS_4 (LPS) and LGPS having conductivities of 1.0×10^{-3} and 6.0×10^{-3} S cm^{-1} at 30 °C, respectively, were prepared.[27]

Figure 1a shows photographs of mixtures of G3-based liquids and sulfide SEs after they were kept for 7 d. For pure G3, the change in color is evident, indicating that both LPS and LGPS dissolved well. Ethers are intrinsically good solvents for LEs because of the donor ability of oxygen to the Lewis-acidic Li^+ ions.[33,37] In other words, ethers are good at dissolving Li salts. However, this also implies the possibility of reaction with and or dissolution of sulfide materials. In this regard, the reaction of sulfide SEs toward pure G3 is not surprising. However, when four moles of G3 are added to 1 mol of Li salt (LiTFSI), forming the solvent–salt complex, $Li(G3)_4$, the dissolution was reduced, as seen in Figure 1a. Further, in the case of equimolar complex of LiG3, the solution appears clear indicating negligible dissolution. Phase analyses were also carried out using X-ray diffraction (XRD) experiments (Figure 1b). Mixtures of the LPS or LGPS powders containing 10 mol% of G3-based liquids were pelletized and stored under Ar for several different time periods, and the XRD patterns of the pellets were obtained. In the case of $Li(G3)_4$, intense peaks of an unidentified phase were observed in the case of LPS (Figure 1b, filled triangle). In contrast, LGPS-$Li(G3)_4$ showed very minor impurity peaks (filled diamond) indicating that the stability of LGPS toward the G3-based LE is superior to that of LPS. In the case of LiG3, no impurity peak was observed for both LPS and LGPS as confirmed by the XRD measurements and shown in Figure 1b. The results of UV–vis molecular absorption spectroscopy and the weight fraction of dissolved elements (obtained by inductively coupled plasma optical emission spectroscopy (ICPOES)) (Figure S1, Supporting Information) also confirm the trends observed in both the visual tests (Figure 1a) and the XRD results (Figure 1b). Most importantly we would like to emphasize that the equimolar complex, LiG3, showed negligible signs of dissolution for both LPS and LGPS.

Figure 1c represents the Nyquist plots obtained using Li-ion blocking cells (Ti/SE/Ti). Note that the changes in resistance over time are smallest when LiG3 is in contact with the SEs, corroborating their excellent stability. As compared to the case for LGPS-$Li(G3)_4$, the LPS-$Li(G3)_4$ exhibits much increased resistance, again indicating more reactivity of LPS toward $Li(G3)_4$ than LGPS. The Arrhenius plots of pure SEs and SE-LiG3 mixture pellets are represented in Figure 1d (the Nyquist plots are shown in Figure S2, Supporting Information). The addition of LiG3 into LPS and LGPS does not significantly degrade conductivity and this system appears to be stable. The stability of LPS and LGPS was also confirmed in another type of solvent–salt complex, $Li(AN)_2TFSI$[31] as seen in Figure S3 (Supporting Information).

Following our success in obtaining the compatible or inert LE (LiG3 and $Li(AN)_2TFSI$) with the sulfide SEs, we would like to offer explanations of the following observations. First, the addition of Li salt significantly suppresses dissolution of SEs. Second, the LGPS exhibits better stability than the LPS. The ethers are important solvents, enabling the reversible operation of Li–S[7] and Li–O_2 batteries.[38] In particular, for Li–S batteries the reason why the ethers have been selected is because the polysulfide anions S_x^- centers do not attack the solvent, in contrast with the side reactions that occur in conventional carbonate-based LEs.[7] The selection of the ether-based LEs can also be rationalized in this respect as well. More importantly, the nonsolvent behaviors of the SILs (or solvent–salt complexes) toward polysulfides in Li–S batteries[31–33] must also be achieved in the present work (toward sulfide SEs). The strong complexation of glyme with Li salts in the salt–solvent complex significantly weakens the donor ability of oxygen, resulting in suppressed dissolution of polysulfides.[31–33] As seen in **Figure 2**, a similar explanation is possible for the reactivity of sulfide SEs because the oxygen in G3 would normally attack the electropositive elements (P and Ge) of the sulfide SEs by nucleophilic attack. The strong coordination of oxygen to Li ions will lessen the nucleophilicity of oxygen, resulting in the significantly reduced reactivity. According to the hard and soft acids and bases (HSAB) theory, small and compact hard acids tend to react preferentially with hard bases, while large and easily polarizable soft acids react with soft bases.[26] The greater air stability of the phosphorus-free As-substituted Li_4SnS_4 than LPS was explained as being due to the presence of the relatively soft acids, Sn and As, which are less reactive toward the hard base, oxygen, than the hard acid, P.[26] Applying the HSAB theory similarly, P is a harder acid than Ge and is considered more vulnerable toward nucleophilic attack by the hard base,

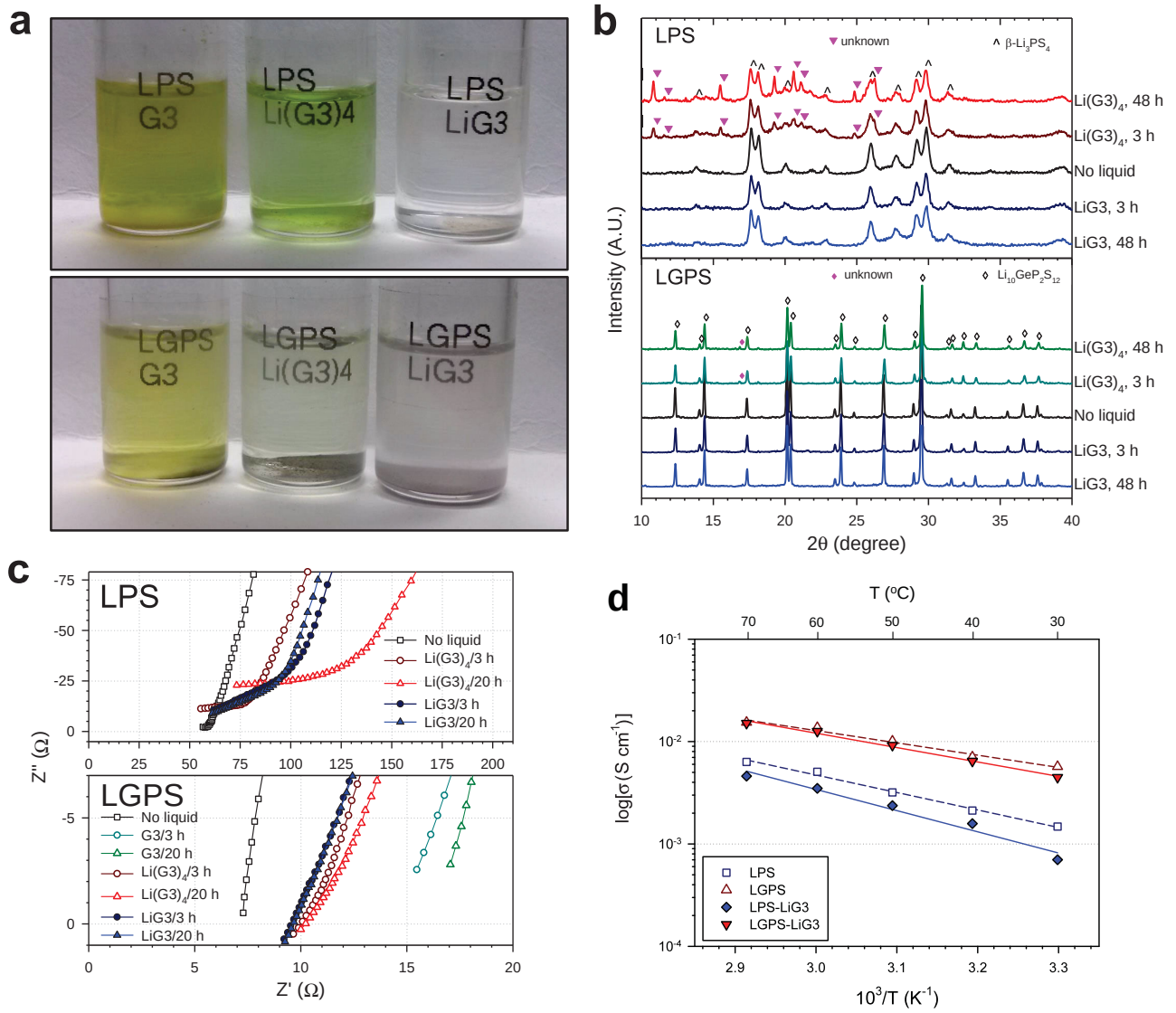

Figure 1. Reactivity of sulfide SEs with glyme-based solvent and solvate ionic liquids (SILs). a) Photographic images of mixtures of LPS or LGPS powders with the liquids (triglyme (G3), $Li(G3)_4$ ($Li(G3)_4TFSI$), and LiG3 (Li(G3)TFSI)) after being kept for 7 d. b) XRD patterns and c) Nyquist plots of LPS and LGPS without and with liquids (G3, $Li(G3)_4$, and LiG3) after being kept for different time periods at 30 °C. d) Arrhenius plots of Li ionic conductivities of LPS and LGPS without and with LiG3 after being kept for 20 h at 30 °C.

oxygen. This might account for the better stability of LGPS over LPS toward the G3 solvent and G3-based LEs.

In spite of our achievements of excellent stability of the sulfide SE toward SIL (LiG3), the physical properties could be degraded by the addition of liquids. **Figure 3**a compares the appearance of the pristine SEs and LiG3-SEs (10 wt% of LiG3). The inclusion of small amounts of LiG3 did not change the SE, and they retained powder-like behaviors. Also, as seen in Figure 3b, LiG3-SE can be made into a pellet by cold-pressing, just as in the case of the pristine SEs. These results clearly confirm the solid behaviors of ASLBs including LiG3. Figure 3c shows the thermal behavior of pristine SEs, LiG3-SEs, and pure LiG3 under Ar. The SIL shows a thermal stability of ≈130 °C. The thermal behavior of the LiG3-SEs is similar to LiG3. This implies that any reactivity between LiG3 and SEs at elevated temperatures of at least 130 °C is also negligible. However, it is true that the inclusion of LiG3 in ASLBs degrades the thermal stability of the pure ASLBs. However, the LiG3-included ASLBs are stable at a much greater temperature than the conventional LIBs (<70 °C).[37] Moreover, further exploration of alternative SILs could widen the thermal window further.[39]

Finally, the feasibility of the inclusion of an SIL (LiG3) into the ASLBs was assessed by using LFP as the electrode material (LFP/Li–In cell). We confirmed in advance that reasonable capacities and reversible cycling of LFP were achievable at 0.1 C (17 mA g^{-1}) by using pure LiG3 as the LE (Figure S4, Supporting Information). As seen in **Figure 4**a, the LFP without LiG3 in all-solid-state cell exhibits negligible capacity at 0.1 C (17 mA g^{-1}) between 2.5 and 4.0 V (vs Li/Li^+) at the second cycle at 30 °C. This result is in line with previous report, where only ≈40 mA h g^{-1} of reversible capacity was obtained at the higher temperature (50 °C), at the extremely low current

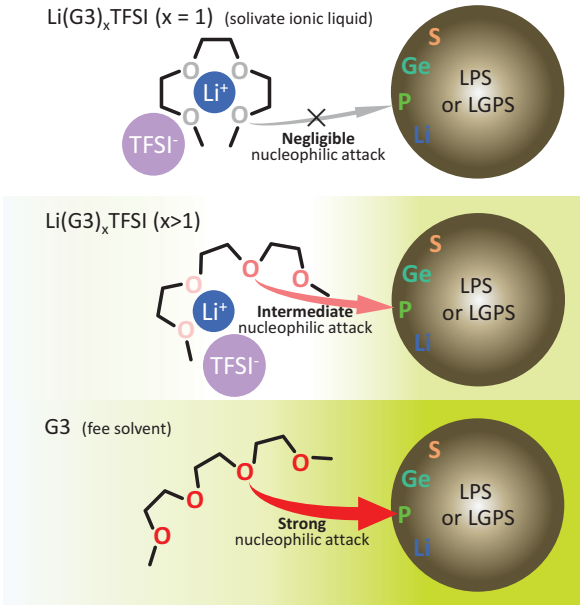

Figure 2. Schematic diagrams representing the reactivity of glyme-based liquids (G3 and $Li(G3)_xTFSI$). Note that strong coordination of Li ions by O in the glyme weakens the nucleophilic attack on electropositive elements, P, resulting in nonsolvent behavior as *x* in $Li(G3)_xTFSI$ decreases.

density (1.3 mA g_{LFP}^{-1} < C/100), and in the wider voltage range (2.0–4.7 V (vs Li/Li^+)) than the conditions in this work.[28] As shown in Figure 4a,b, the LFP electrode that has an LiG3 content of 5.7 wt% shows, in sharp contrast, a reversible capacity of 144 mA h g^{-1}, close to the value which is routinely obtained by the conventional LE-based cells.[40] A similar improvement was also confirmed for the all-solid-state cell using LTO. The reversible capacity of LTO/Li–In cell at 0.2 C (35 mA g_{LTO}^{-1}) in the second cycle increased from 89 to 127 mA h g^{-1} by including 5.0 wt% LiG3 in the electrode (Figure S5, Supporting Information). The results of conventional LTO/Li half-cell using pure LiG3 as the LE are also shown in Figure S6 (Supporting Information).

Figure 4c shows a schematic of the microstructures of the composite electrode layers without and with LiG3. Because cold-pressing is not sufficient to form a poreless monolith, defects in contacts are inevitable. **Table 1** represents the porosities of the cold-pressed SE layers and the composite electrodes obtained by calculating absolute specific densities and measured densities (see the Supporting Information). As expected, the porosities of the SE layers and of typical composite electrodes without liquid are 14%–17% and 28%–40%, respectively. The inclusion of an LE (LiG3) appeared to significantly decrease the porosities by 6.3% point and 11.6% point for LTO and LFP electrodes, respectively. This implies that LiG3 wets or occupies the

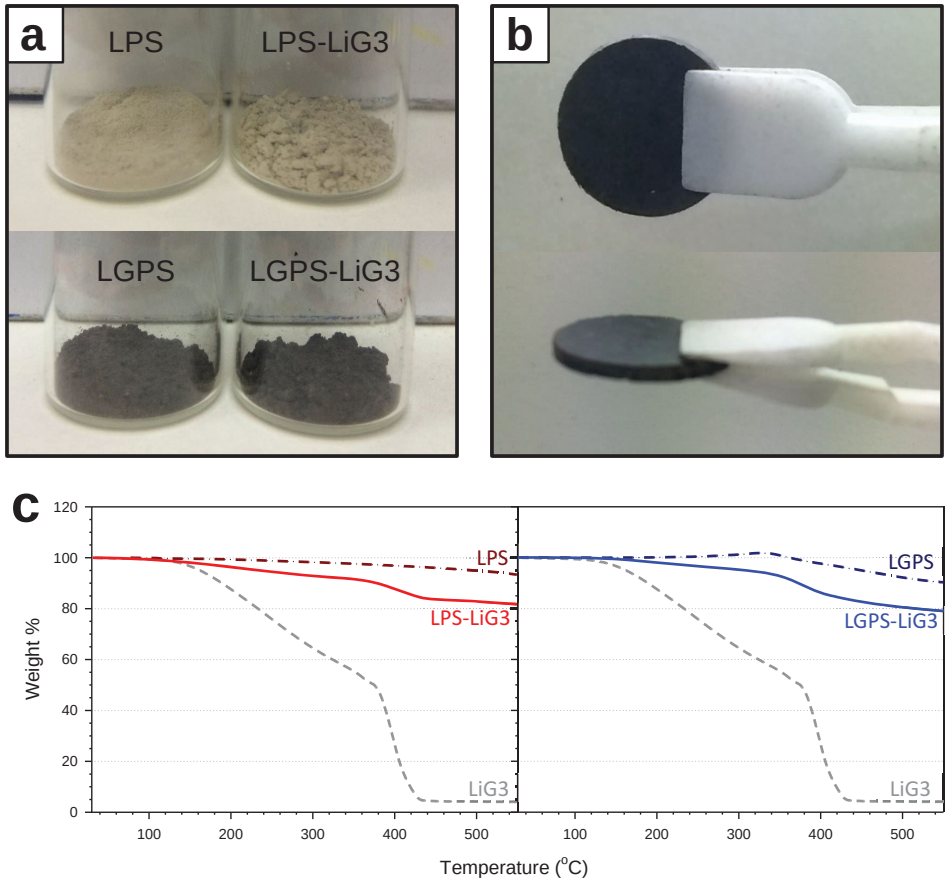

Figure 3. Characteristics of SE-LiG3. a) Photographs of pristine SE and SE-LiG3 powders. b) Photographs of LGPS-LiG3 pellet. c) Thermogravimetric analysis (TGA) profiles of LiG3, the pristine SEs, and SE-LiG3 under Ar.

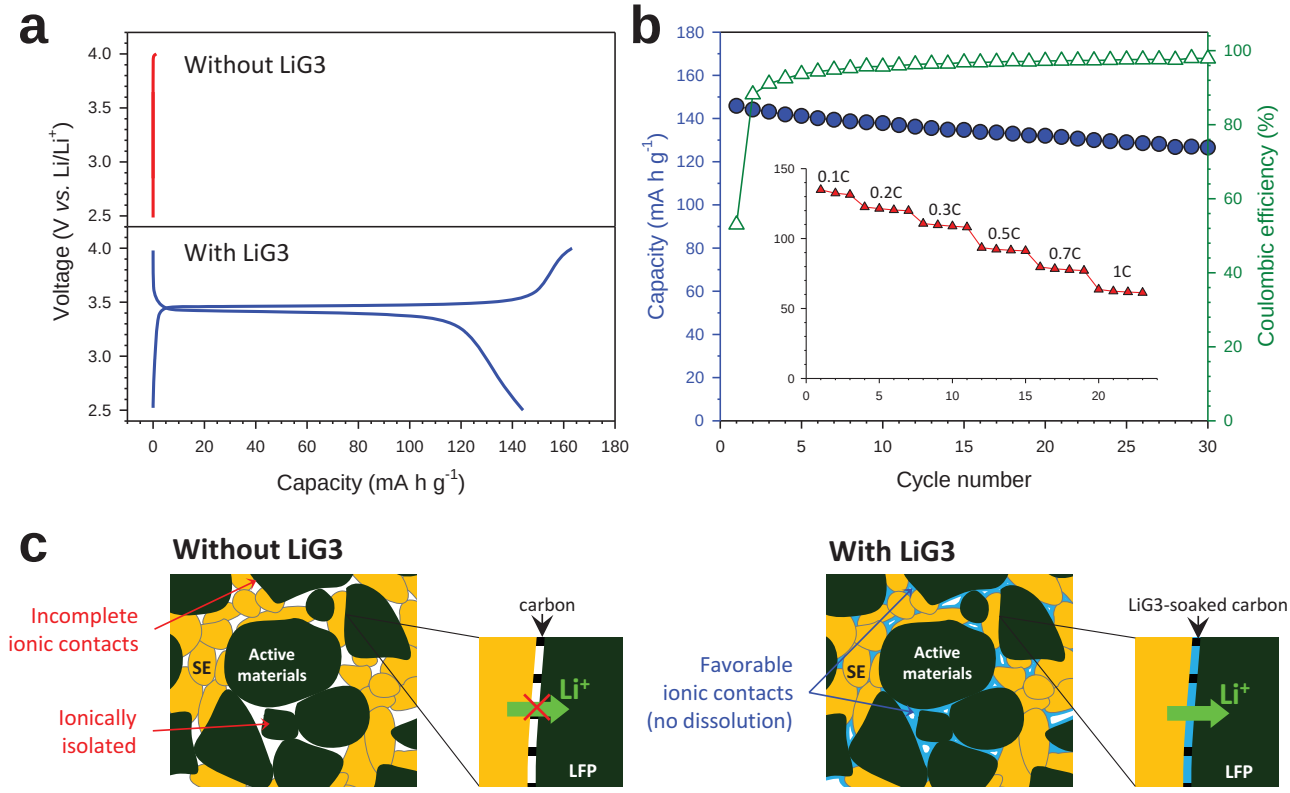

Figure 4. a) Second charge–discharge voltage profiles and b) cycling performance of $LiFePO_4$/Li–In all-solid-state cells without and with LiG3 at 0.1 C (17 mA g_{LFP}^{-1}) at 30 °C. The rate performance is shown in the inset. c) Schematic diagram representing the microstructure of the composite electrodes without and with LiG3, showing that LiG3 improves the imperfect solid–solid contacts. Carbon additives included in the composite electrode are not shown in the scheme.

surroundings of the pores and thus could improve the solid–solid ionic contacts between the active materials and SEs; this is illustrated in Figure 4c. Notably, the extremely poor capacity of LFP in the all-solid-state cell without LiG3 is believed to be due to ionically insulating carbon coating layers as well as the imperfection in SE-LFP contacts. As confirmed by high-resolution transmission electron microscopy (HRTEM) and energy dispersive X-ray spectroscopy (EDS) analysis (Figure S7, Supporting Information), the commercial-grade LFP powders used include a conformal carbon coating layer on the surface. This layer is necessary for electrical wiring of the insulating LFP.[40] However, in the operation voltage range for LFP the carbon coating layer might not act as Li-ion conductor. The carbon coating layer is not troublesome in the LE cells because LEs can easily soak through any defect sites of the carbon coating layer;[41] however, it can act as ion blocking layer in all-solid-state cells because the SE cannot make ionic conduction pathways that penetrate through the carbon coating.[27,42] This could be the reason why the LFP in the all-solid-state cell that did not contain LiG3 shows negligible capacity (Figure 4a). In order to verify the ion blocking by carbon coating layer on LFP in all-solid-state cell, two symmetric Li-ion blocking cells without and with LiG3 (Ti/LGPS/C/LGPS/Ti and Ti/LGPS/(C-LiG3)/LGPS/Ti) were prepared as shown in Figure S8a (Supporting

Table 1. Porosity data of cold-pressed SE and composite electrode pellets without and with addition of LiG3.

Sample name	Presence of LiG3	Weight ratio [wt%]	Volume of LiG3 [μL cm^{-2}]	Porosity [%]
LPS	X	–	–	14
LPS-LiG3	O	90:10 (LPS:LiG3)	–	–2.7
LGPS	X	–	–	17
LGPS-LiG3	O	90:10 (LGPS:LiG3)	–	–3.6
LTO-LPS-C	X	49.8:49.8:0.5 (LTO:LPS:C)	–	27.5
LTO-LPS-C-LiG3	O	49.8:44.8:0.5:5.0 (LTO:LPS:C:LiG3)	0.52	20.2
LFP-LGPS-C	X	37.7:56.6:5.7 (LFP:LGPS:C)	–	40.4
LFP-LGPS-C-LiG3	O	37.7:50.9:5.7:5.7 (LFP:LGPS:C:LiG3)	0.30	28.8

Information) and tested by AC impedance method. As seen in Figure S8b (Supporting Information), the Ti/LGPS/C/LGPS/Ti cell without LiG3 showed noisy signal when the applied pressure for the cell is low. In sharp contrast, the Ti/LGPS/(C-LiG3)/LGPS/Ti cell including LiG3 exhibited the nice semicircle followed by the Warburg tail. Consistently, when applied pressure was increased (Figure S8c, Supporting Information), the wet Ti/LGPS/(C-LiG3)/LGPS/Ti cell with LiG3 showed much smaller (more than ten times smaller) semicircle than the dry Ti/LGPS/C/LGPS/Ti cell. These results strongly support that LiG3 paves the favorable ionic conduction pathways in between the LFP and SE domains without causing significant side reactions, and results in achieving close to the theoretical capacity (170 mA h g^{-1}) of LFP in ASLBs. It is also noted that, even after the addition of LiG3, the porosities of LFP and LTO composite electrodes with LiG3 are still not zero (LFP electrode: 28.8%, LTO electrode: 20.2%) as seen in Table 1. In this regard, it is reasonable to consider that the LiG3 alone cannot deliver all Li^+ ions required to exhibit the capacities for LFP and LTO close to the theoretical ones, and thus the SE in composite electrodes still acts as the ionic conduction pathways in the composite electrode as well.

In conclusion, the excellent stability of sulfide SEs with the SIL (LiG3) and their application in high-performance ASLBs were successfully demonstrated. The underlying physics of significantly reduced reactivity of the oxygen in G3 toward nucleophilic attack on the SEs explains the compatibility or inertness of LiG3 with the SEs of LPS and LGPS. Additionally, the better stability of LGPS than LPS toward $Li(G3)_xTFSI$ was rationalized by using the HSAB theory. Finally, significantly increased capacities of ASLBs containing LFP (144 mA h g^{-1}) by addition of a small amount (5.7 wt%) of LiG3 were shown, which is dramatically contrasted by a negligible capacity without addition of LiG3. This increase in capacity is due to the additional ionic pathways paved by the LiG3. We believe that our results are not only a breakthrough as a design concept in high-performance ASLBs, but can also provide motivation for in-depth understanding of the interfacial reactivity in various battery systems.

Experimental Section

Preparation of Materials: LPS powders were prepared by mechanical milling a stoichiometric mixture of Li_2S (99.9%, Alfa Aesar) and P_2S_5 (99%, Sigma Aldrich) powders, followed by heat treatment at 243 °C for 1 h.[27] LGPS powders were prepared by heat treatment of a pelletized stoichiometric mixture of Li_2S, P_2S_5, and GeS_2 (99.9%, American Elements) at 550 °C for 10 h.[27] The solvate ionic liquids were prepared by dissolving a stoichiometric amount of LiTFSI (99.95%, Sigma Aldrich) into anhydrous triglyme (G3) (99%, Sigma Aldrich). The G3 were dried by using CaH_2 (95%, Sigma Aldrich) before use.

Material Characterization: For the visual tests on reactivity of SE with the glyme-based liquids, SE powder (10 mg) was added into liquid (2.0 mL), and then kept for 7 d under Ar. For the measurements of structural and conductivity changes of SE pellets upon exposure to the glyme-based liquids, the as-prepared SE pellets that contained 10 mol% of liquid were stored under Ar for different designated times. XRD cells which contain hermetically sealed SE powders with a beryllium window were mounted on a D8-Bruker Advance diffractometer equipped with CuKα radiation (1.54056 Å). All the XRD patterns were recorded at 40 kV and 40 mA using a continuous scanning mode at 1.5° min^{-1}. The thermogravimetric analysis (TGA) experiments were carried out from 25 to 600 °C at 5 °C min^{-1} under Ar using a Q50 (TA Instrument Corp.).

Electrochemical Characterization: In order to obtain Li-ion conductivity, Li-ion blocking cell of Ti/SE/Ti was subjected to AC method using an Iviumstat (IVIUM Technologies Corp.) with an amplitude of 10 mV and a frequency range from 1.5 MHz to 10 Hz. All-solid-state cells were fabricated as the following: Composite electrodes were prepared by mixing the active materials, SE powders, conductive carbon additives (super P), and solvate ionic liquids with the targeted weight ratio which is shown in Table 1. $Li_{0.5}In$ prepared by mixing In (Aldrich, 99%) and Li (FMC Lithium Corp.) powders was used as the counter and reference electrode material. After SE layer was formed by pelletizing 150 mg of the SE by pressing at 74 MPa, 10 mg of the as-prepared composite electrodes were spread, followed by pressing at 370 MPa. Then, 100 mg of the as-prepared $Li_{0.5}In$ was attached on the other side of SE layer by pressing at 370 MPa. All procedures were performed in a polyaryletheretherketone (PEEK) mold (diameter = 1.3 cm) with two Ti metal rods as current collectors. All the processes for preparing the SEs and fabricating the all-solid-state cells were performed in an Ar-filled dry box. Galvanostatic charge–discharge cycling test for LFP all-solid-state cell was performed at 30 °C at 17 mA g^{-1} (50 μA cm^{-2}, 0.1 C).

Supporting Information

Supporting Information is available from the Wiley Online Library or from the author.

Acknowledgements

This work was supported by the Energy Efficiency & Resources Program of the Korea Institute of Energy Technology Evaluation and Planning (KETEP) grant funded by the Korea government Ministry of Trade, Industry & Energy (No. 20112010100150), by Basic Science Research Program through the National Research Foundation of Korea (NRF) funded by the Ministry of Education (No. NRF-2014R1A1A2058760), and by the 2015 Research Fund (1.150034.01) of UNIST. The authors thank Dr. Kevin Leung for helpful discussions of the theoretical considerations.

Received: May 1, 2015
Revised: June 19, 2015
Published online: August 3, 2015

[1] J. B. Goodenough, Y. Kim, *Chem. Mater.* **2010**, *22*, 587.
[2] J.-M. Tarascon, *Philos. Trans. R. Soc. A* **2010**, *368*, 3227.
[3] N. Kamaya, K. Homma, Y. Yamakawa, M. Hirayama, R. Kanno, M. Yonemura, T. Kamiyama, Y. Kato, S. Hama, K. Kawamoto, A. Mitsui, *Nat. Mater.* **2011**, *10*, 682.
[4] A. Hayashi, K. Noi, A. Sakuda, M. Tatsumisago, *Nat. Commun.* **2012**, *3*, 856.
[5] Y. S. Jung, D. Y. Oh, Y. J. Nam, K. H. Park, *Isr. J. Chem.* **2015**, *55*, 472.
[6] Y. Lu, J. B. Goodenough, Y. Kim, *J. Am. Chem. Soc.* **2011**, *133*, 5756.
[7] P. G. Bruce, S. A. Freunberger, L. J. Hardwick, J.-M. Tarascon, *Nat. Mater.* **2012**, *11*, 19.
[8] Y. Zhao, L. Wang, H. R. Byon, *Nat. Commun.* **2013**, *4*, 1896.
[9] J. Fu, *J. Mater. Sci.* **1998**, *33*, 1549.
[10] R. Murugan, V. Thangadurai, W. Weppner, *Angew. Chem., Int. Ed.* **2007**, *46*, 7778.
[11] C. Ma, E. Rangasamy, C. Liang, J. Sakamoto, K. L. More, M. Chi, *Angew. Chem., Int. Ed.* **2015**, *54*, 129.
[12] Y. J. Nam, S. J. Jo, D. Y. Oh, J. M. Im, S. Y. Kim, J. H. Song, Y.-G. Lee, S.-Y. Lee, Y. S. Jung, *Nano Lett.* **2015**, *15*, 3317.
[13] Z. Lin, Z. Liu, W. Fu, N. J. Dudney, C. Liang, *Angew. Chem., Int. Ed.* **2013**, *52*, 7460.

[14] T. A. Yersak, H. A. Macpherson, S. C. Kim, V.-D. Le, C. S. Kang, S.-B. Son, Y.-H. Kim, J. E. Trevey, K. H. Oh, C. Stoldt, S.-H. Lee, *Adv. Energy Mater.* **2013**, *3*, 120.
[15] B. R. Shin, Y. J. Nam, J. W. Kim, Y.-G. Lee, Y. S. Jung, *Sci. Rep.* **2014**, *4*, 5572.
[16] B. Wang, J. B. Bates, F. X. Hart, B. C. Sales, R. A. Zuhr, J. D. Robertson, *J. Electrochem. Soc.* **1996**, *143*, 3203.
[17] S. Stramare, V. Thangadurai, W. Weppner, *Chem. Mater.* **2003**, *15*, 3974.
[18] S. Ohta, J. Seki, Y. Yagi, Y. Kihira, T. Tani, T. Asoka, *J. Power Sources* **2014**, *265*, 40.
[19] K. H. Kim, Y. Iriyama, K. Yamamoto, S. Kumazaki, T. Asaka, K. Tanabe, C. A. J. Fisher, T. Hirayama, R. Murugan, Z. Ogumi, *J. Power Sources* **2011**, *196*, 764.
[20] M. Kotobuki, H. Munakata, K. Kanamura, Y. Sato, T. Yoshida, *J. Electrochem. Soc.* **2010**, *157*, A1076.
[21] A. Sakuda, A. Hayashi, M. Tatsumisago, *Sci. Rep.* **2013**, *3*, 2261.
[22] P. Bron, S. Johansson, K. Zick, J. S. auf der Guenne, S. Dehnen, B. Roling, *J. Am. Chem. Soc.* **2013**, *135*, 15694.
[23] F. Mizuno, A. Hayashi, K. Tadanaga, M. Tatsumisago, *Adv. Mater.* **2005**, *17*, 918.
[24] Y. Seino, T. Ota, K. Takada, A. Hayashi, M. Tatsumisago, *Energy Environ. Sci.* **2014**, *7*, 627.
[25] H. Muramatsu, A. Hayashi, T. Ohtomo, S. Hama, M. Tatsumisago, *Solid State Ionics* **2011**, *182*, 116.
[26] G. Sahu, Z. Lin, J. Li, Z. Liu, N. Dudney, C. Liang, *Energy Environ. Sci.* **2014**, *7*, 1053.
[27] B. R. Shin, Y. J. Nam, D. Y. Oh, D. H. Kim, J. W. Kim, Y. S. Jung, *Electrochim. Acta* **2014**, *146*, 395.
[28] A. Sakuda, H. Kitaura, A. Hayashi, M. Tatsumisago, Y. Hosoda, T. Nagakane, A. Sakamoto, *Chem. Lett.* **2012**, *41*, 260.
[29] H. Kitaura, A. Hayashi, K. Tadanaga, M. Tatsumisago, *J. Electrochem. Soc.* **2009**, *156*, A114.
[30] B. R. Shin, Y. S. Jung, *J. Electrochem. Soc.* **2014**, *161*, A154.
[31] M. Cuisinier, P.-E. Cabelguen, B. D. Adams, A. Garsuch, M. Balasubramanian, L. F. Nazar, *Energy Environ. Sci.* **2014**, *7*, 2697.
[32] L. Suo, Y.-S. Hu, H. Li, M. Armand, L. Chen, *Nat. Commun.* **2013**, *4*, 1481.
[33] K. Dokko, N. Tachikawa, K. Yamauchi, M. Tsuchiya, A. Yamazaki, E. Takashima, J.-W. Park, K. Ueno, S. Seki, N. Serizawa, M. Watanabe, *J. Electrochem. Soc.* **2013**, *160*, A1304.
[34] C. A. Angell, Y. Ansari, Z. Zhao, *Faraday Discuss.* **2012**, *154*, 9.
[35] T. Tamura, T. Hachida, K. Yoshida, N. Tachikawa, K. Dokko, M. Watanabe, *J. Power Sources* **2010**, *195*, 6095.
[36] K. Yoshida, M. Nakamura, Y. Kazue, N. Tachikawa, S. Tsuzuki, S. Seki, K. Dokko, M. Watanabe, *J. Am. Chem. Soc.* **2011**, *133*, 13121.
[37] K. Xu, *Chem. Rev.* **2004**, *104*, 4303.
[38] L. Johnson, C. Li, Z. Liu, Y. Chen, S. A. Freunberger, P. C. Ashok, B. B. Praveen, K. Dholakia, J.-M. Tarascon, P. G. Bruce, *Nat. Chem.* **2014**, *6*, 1091.
[39] K. Ueno, K. Yoshida, M. Tsuchiya, N. Tachikawa, K. Dokko, M. Watanabe, *J. Phys. Chem. B* **2012**, *116*, 11323.
[40] B. L. Ellis, K. T. Lee, L. F. Nazar, *Chem. Mater.* **2010**, *22*, 691.
[41] F.-S. Li, Y.-S. Wu, J. Chou, M. Winter, N.-L. Wu, *Adv. Mater.* **2015**, *27*, 130.
[42] J. E. Trevey, C. R. Stoldt, S.-H. Lee, *J. Electrochem. Soc.* **2011**, *158*, A1282.

